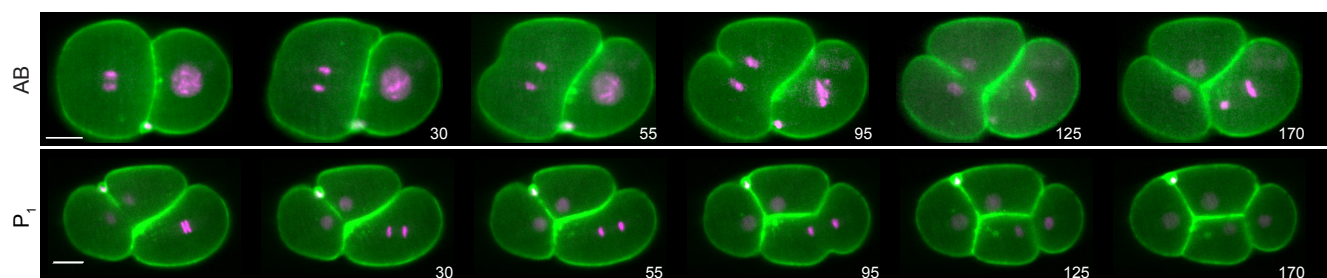
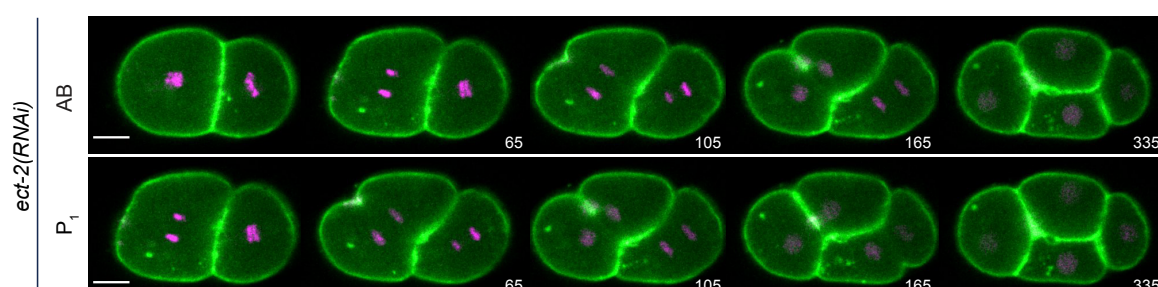


Figure S1

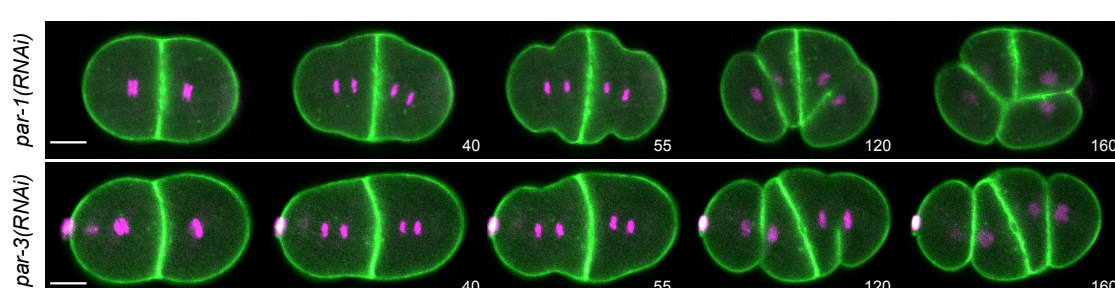
A



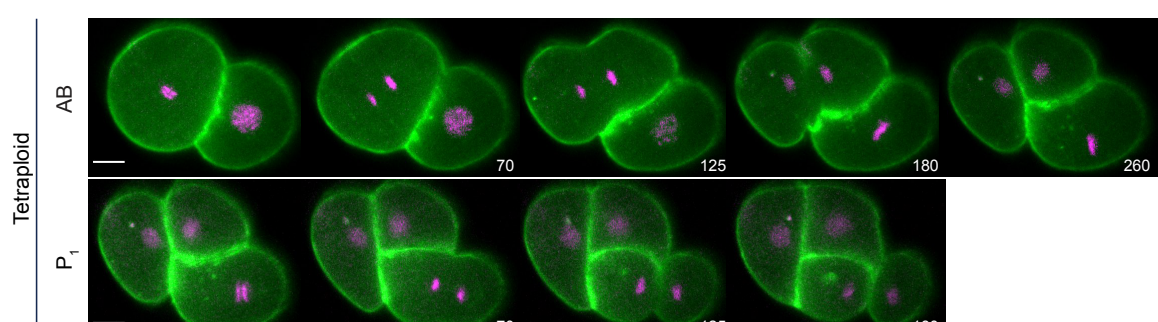
B



C



D



E

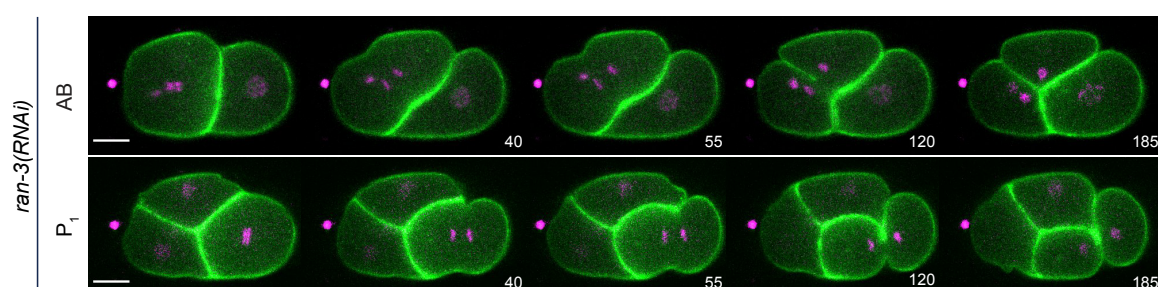


Fig. S1. Comparison of cytokinesis in AB and P₁ cells. Timelapse images of A) control (also shown in Figure 1A), B) ect-2(RNAi), C) par-1(RNAi) (top) and par-3(RNAi) (bottom), D) tetraploid and E) ran-3(RNAi) embryos co-expressing mCherry::HIS-58; GFP::PH (A, E) or mCherry::HIS-58 and mNeonGreen::PH (B-D). All scale bars are 10 μm.

Figure S2

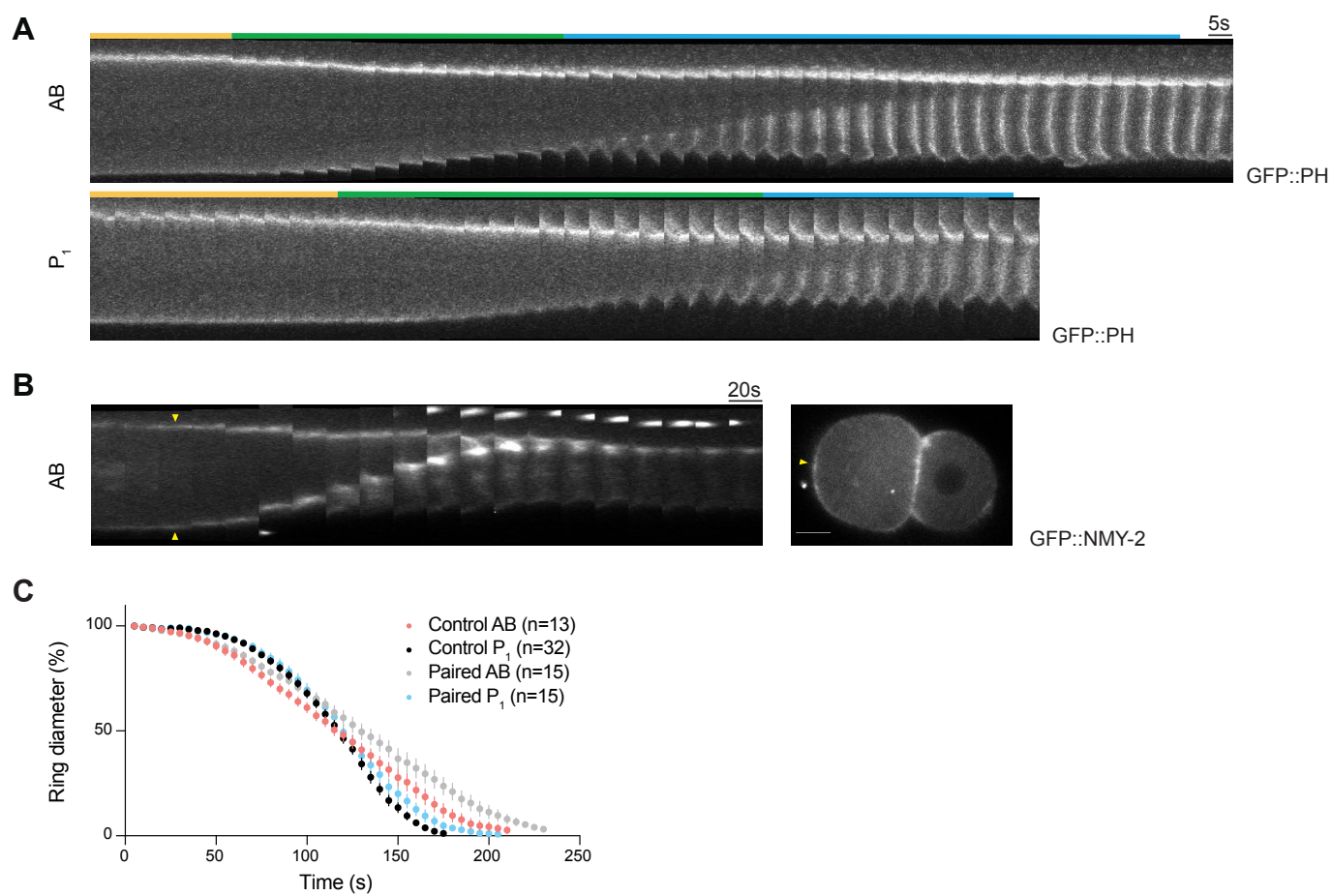


Fig. S2. AB and P₁ cells have distinct cytokinesis phases. A) Kymographs were generated from the furrow region in AB (top) and P₁ (bottom) cells, from images acquired at 5-second intervals from anaphase onset until closure. The bars indicate the duration of ring assembly (yellow), furrow initiation (green) and ring constriction (yellow) phases. B) Left: a kymograph was generated from a cell expressing GFP::NMY-2, from images acquired at 20-second intervals. Right: image shows myosin localization during ring assembly, before furrow initiation. Yellow arrowheads point to myosin accumulation. C) A graph shows average ring closure in control AB and P₁ cells (shown in main figures) compared to paired (*i.e.* sister cells from the same embryo) AB and P₁ cells. The sample sizes are indicated (n) and error bars show s.e.m.

Figure S3

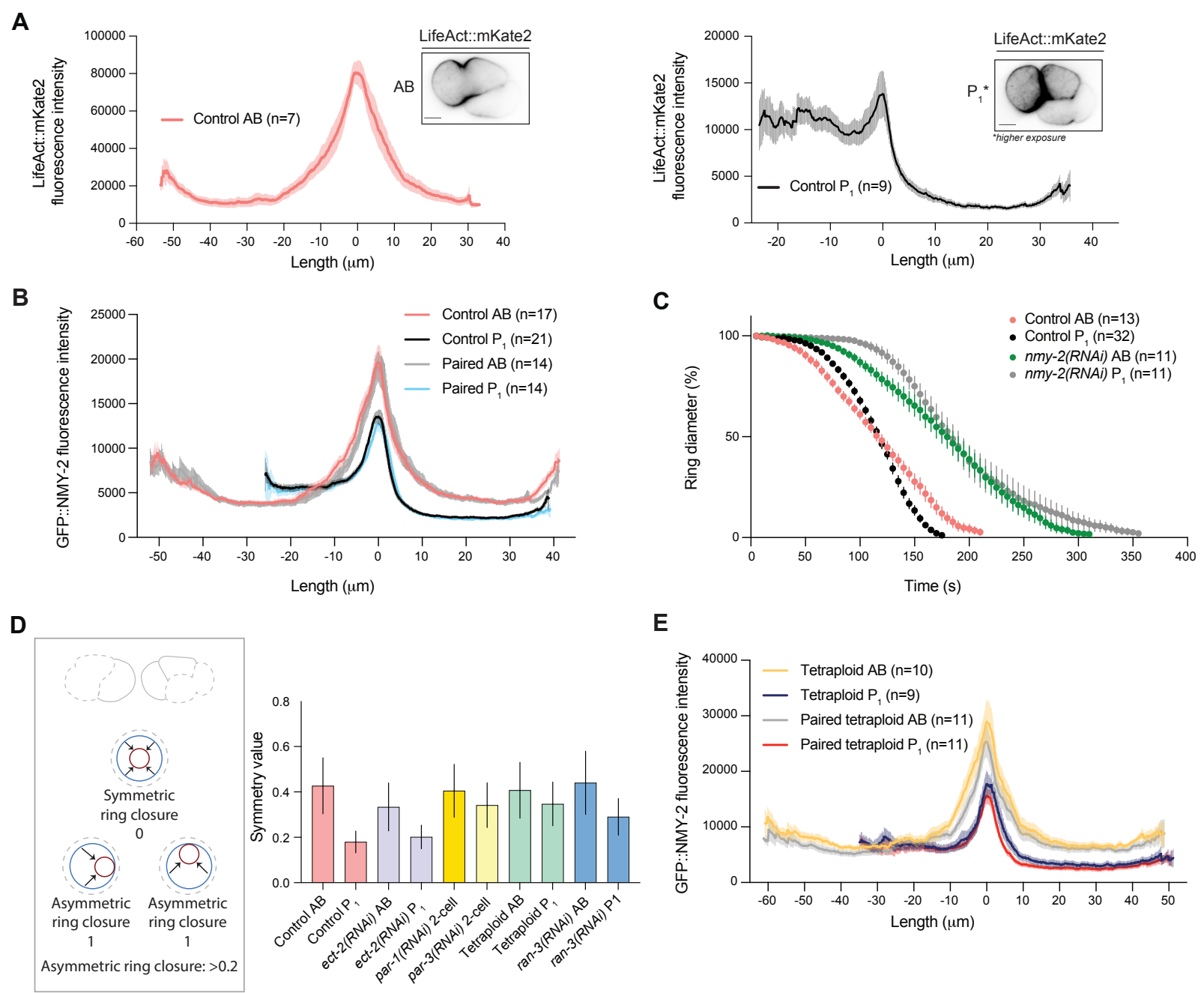
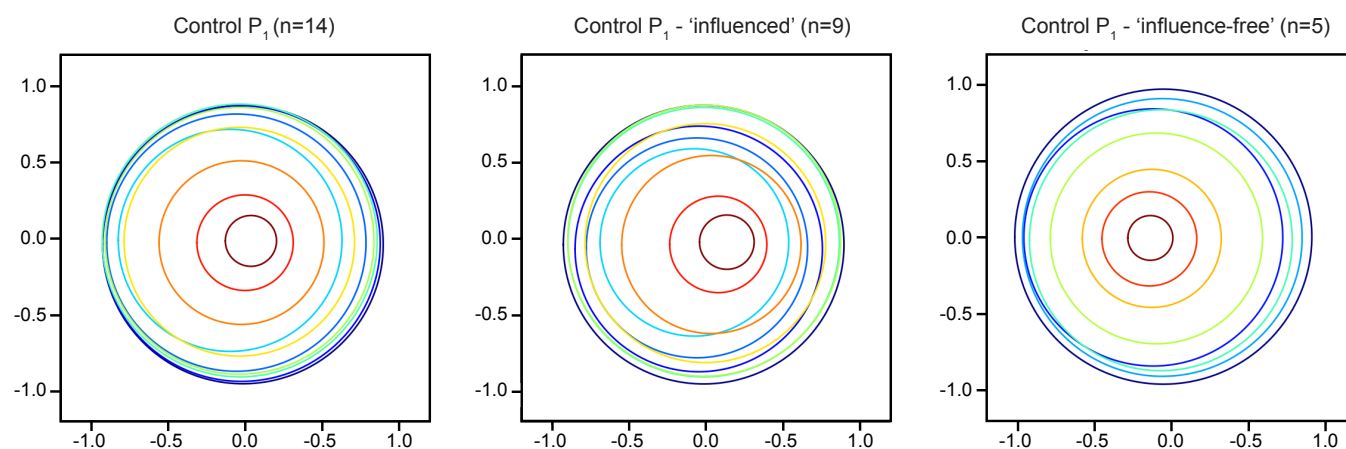


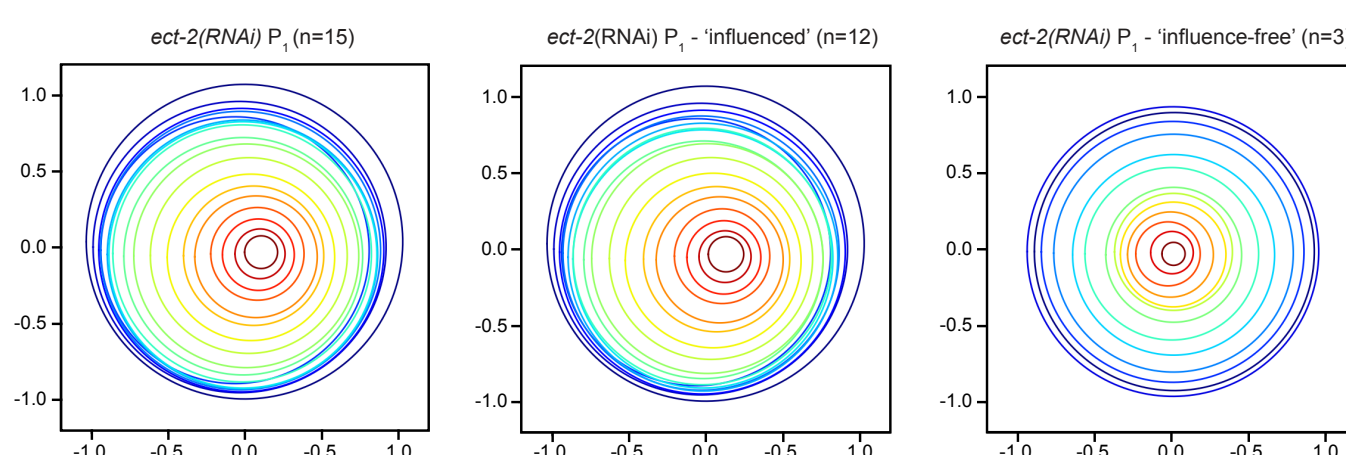
Fig. S3. Characterization of cytokinesis shows differences in actomyosin, and asymmetric ring closure in AB and P₁ cells. A) Inverted images show LifeAct::mKate2 localization in control AB and P₁ cells. Graphs show the average accumulation of LifeAct::mKate2 at the midplane cortex of AB (left) and P₁ (right) cells. B) A graph shows GFP::NMY-2 levels at the midplane cortex of control AB and P₁ cells (shown in main figures) compared to paired cells. C) A graph shows ring closure in *nmy-2(RNAi)* AB and P₁ cells compared to control. D) Left: Cartoon embryos and end-on views show how the symmetry of ring closure was quantified. Values closer to 1 are asymmetric (along the x or y-axis), while those closest to 0 are symmetric. Right: graph shows the symmetry measurements for control embryos, after *ect-2*, *par-1*, *par-3* or *ran-3(RNAi)*, and in tetraploid embryos. E) A graph shows GFP::NMY-2 levels at the midplane cortex of tetraploid AB and P₁ cells (shown in main figures) compared to paired tetraploid cells. For all graphs, n's are indicated, and error bars show s.e.m. All scale bars are 10 μm .

Figure S4

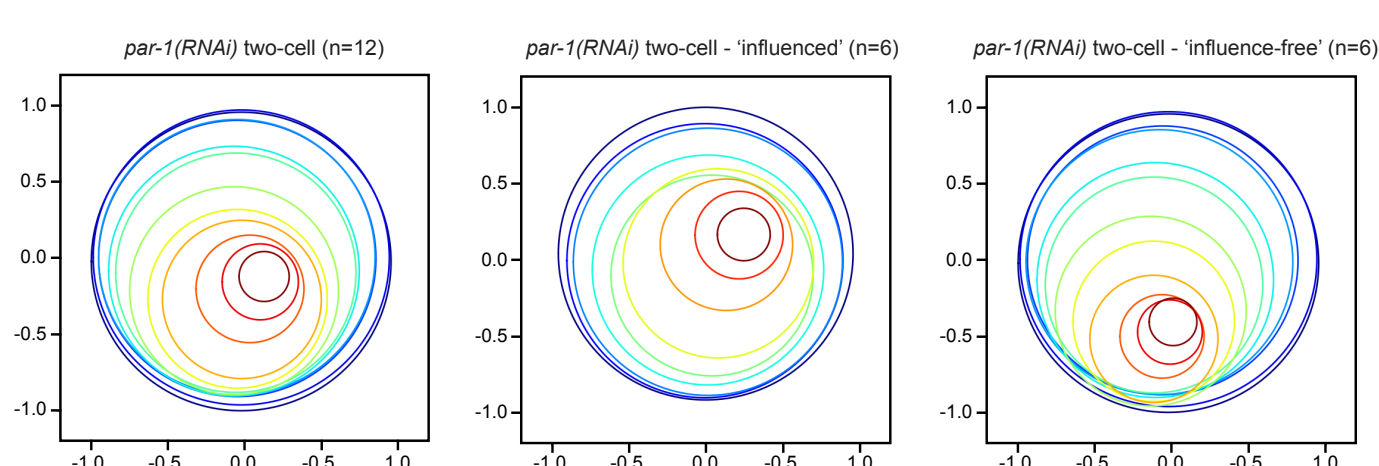
A



B



C



D

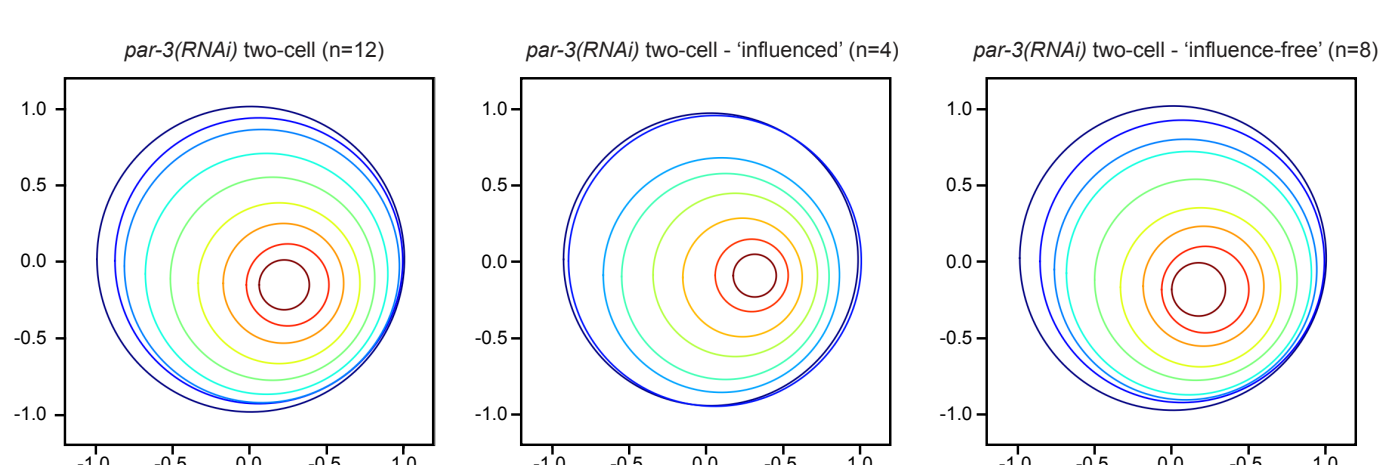


Fig. S4. Symmetry of ring closure is similar between influenced and influence-free P₁ cells.

Ring closure is shown over time for A) control, B) *ect-2(RNAi)*, C) *par-1(RNAi)*, and D) *par-3(RNAi)* P₁ cells, with each timepoint as a different color. Average ring closure for all n's is shown in the left column. The middle column is the average ring closure for influenced P₁ cells, and the right column is the average ring closure for influence-free P₁ cells. The x and y-axis indicate ratios of the distance from the starting position (0).

Figure S5

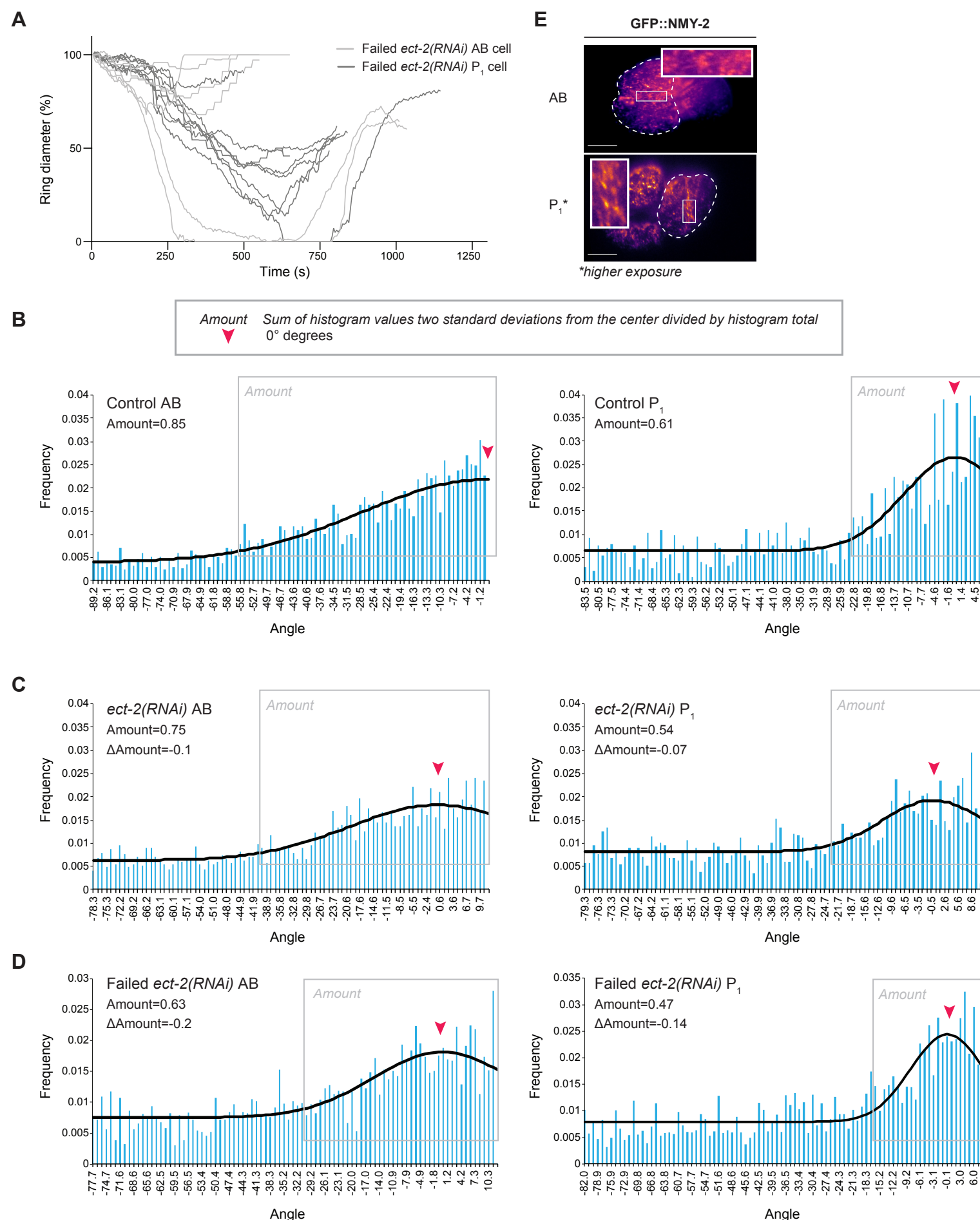


Fig. S5. Myosin filaments are less-well organized and aligned in *ect-2(RNAi)* AB and P₁ cells. A) A graph shows partial ring closure and regression for *ect-2(RNAi)* AB and P₁ cells that fail cytokinesis. B-D) Histograms show the frequency distribution (y-axis) of myosin filament bundles at different angles (x-axis) in AB and P₁ cells. Measurements were taken in the furrow region of B) control cells (shown in Figure 1E), C) *ect-2(RNAi)* cells that complete cytokinesis (shown in Figure 2H) and D) *ect-2(RNAi)* cells that fail cytokinesis (shown in Figure S5E). Well-aligned filament bundles are close to 0° (red arrowhead). The proportion of filament bundles within two standard deviations of the highest frequency peak, outlined by the grey boxes, is indicated as ‘Amount’ on each graph. E) Pseudocolored HILO images show GFP::NMY-2 in *ect-2(RNAi)* AB and P₁ cells (outlined by the dashed line) that fail cytokinesis.

Figure S6

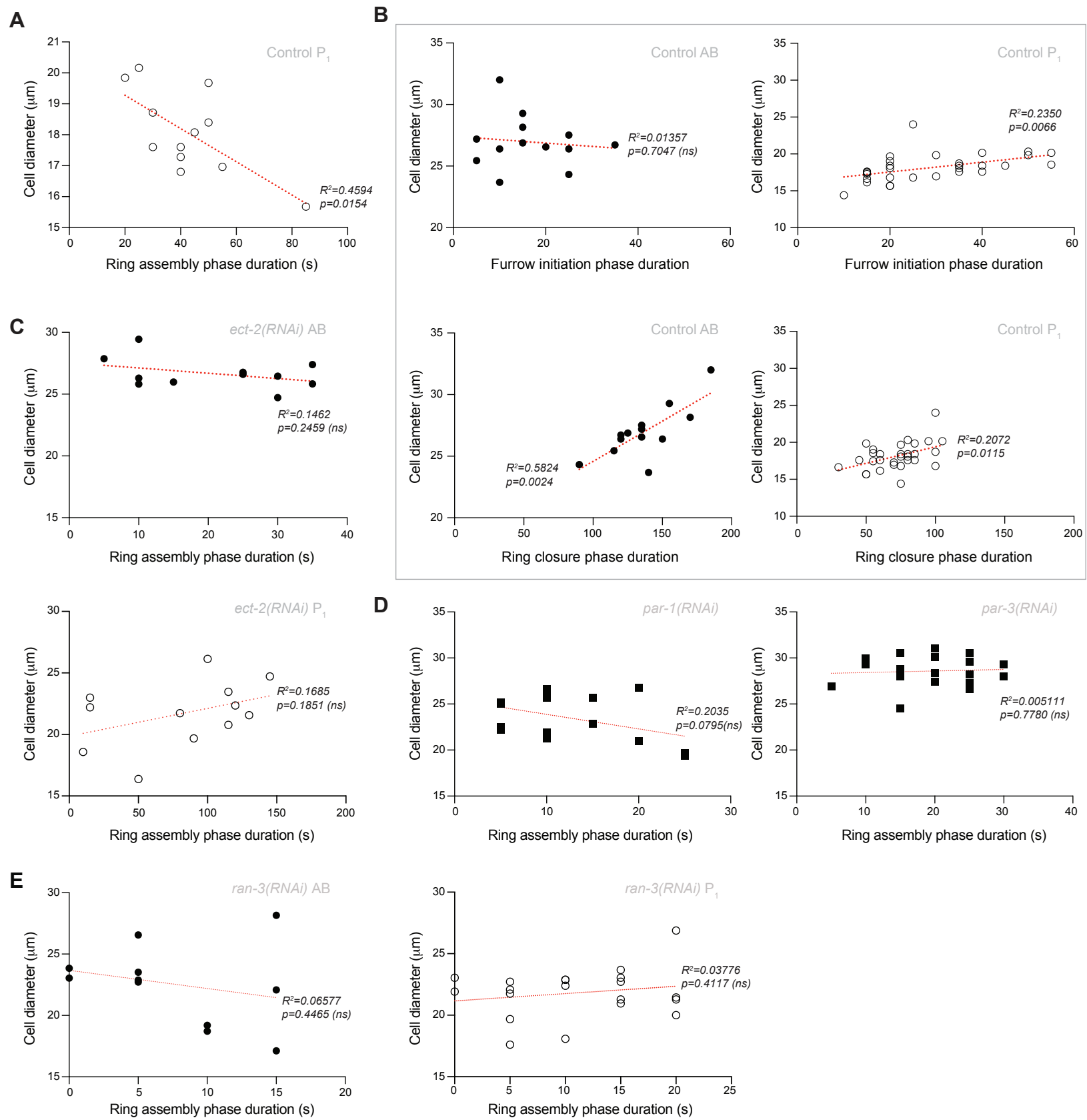


Fig. S6. There is no correlation between the duration of ring assembly and cell size after ECT-2 depletion, disruption of cell fate or lowering Ran-GTP in P₁ cells. A) A graph shows the correlation between the duration of ring assembly and diameter for twelve randomly selected P₁ cells. B) Graphs show the correlation between the duration of furrow initiation (top) or ring closure (bottom) phases and cell diameter. C) Graphs show the correlation between the duration of ring assembly and diameter for AB (top) and P₁ (bottom) cells in *ect-2(RNAi)* cells. D) Graphs show the correlation between the duration of ring assembly and diameter for *par-1(RNAi)* (left) and *par-3(RNAi)* (right) P₀ daughter cells. D) Graphs show the correlation between the duration of ring assembly and diameter for AB (left) and P₁ (right) cells in *ran-3(RNAi)* cells. For all graphs, the red lines show simple linear regression (R^2 and p are shown; ns is not significant).

Figure S7

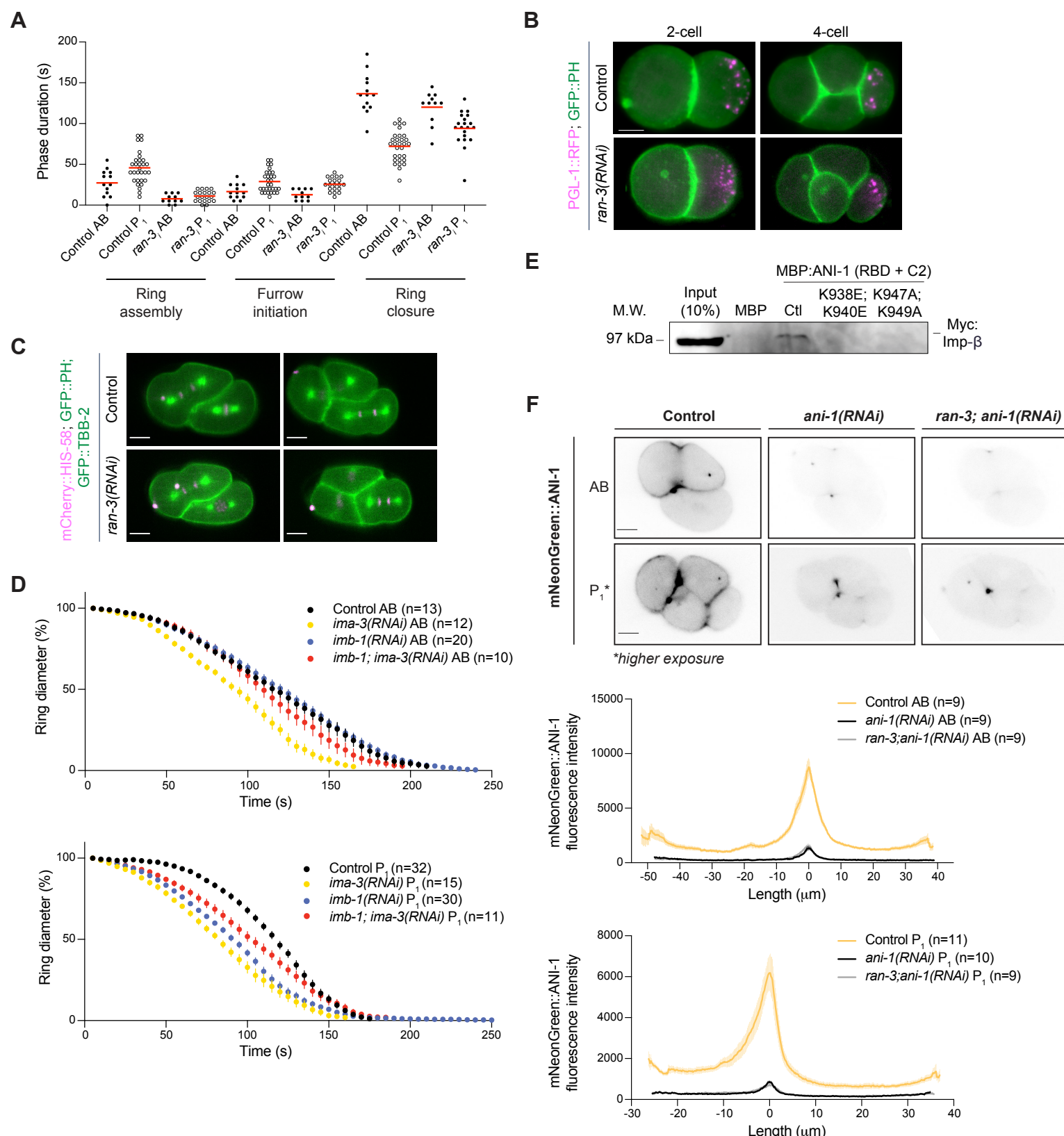
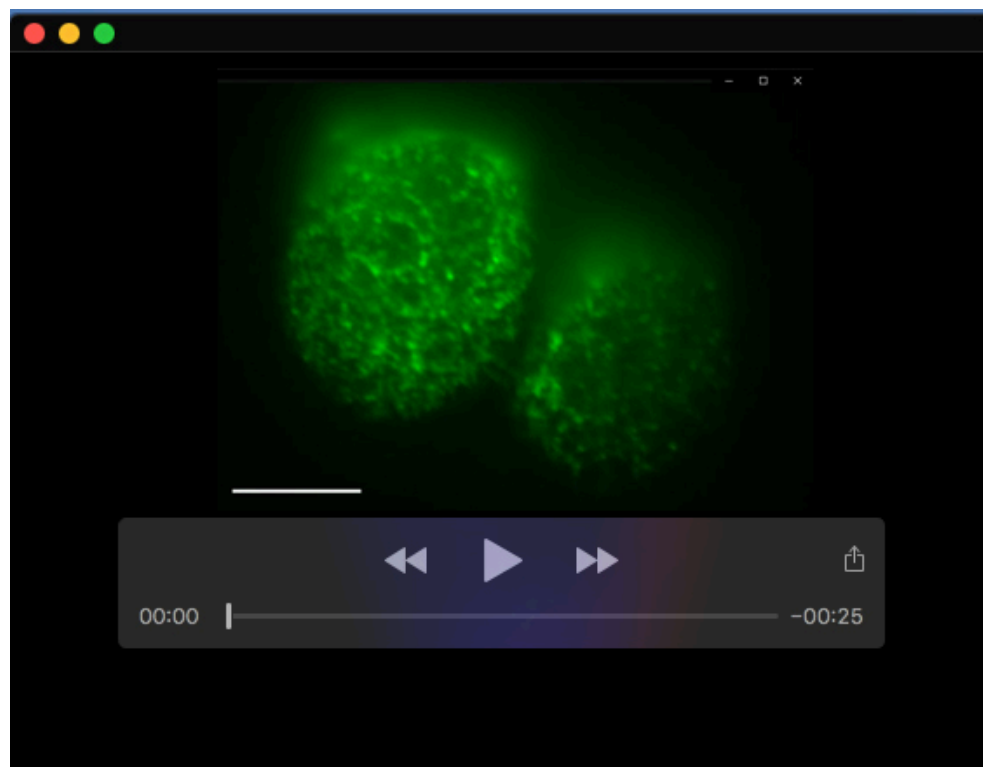


Fig. S7. Different thresholds of importin- α and - β control cytokinesis in AB and P₁ cells.

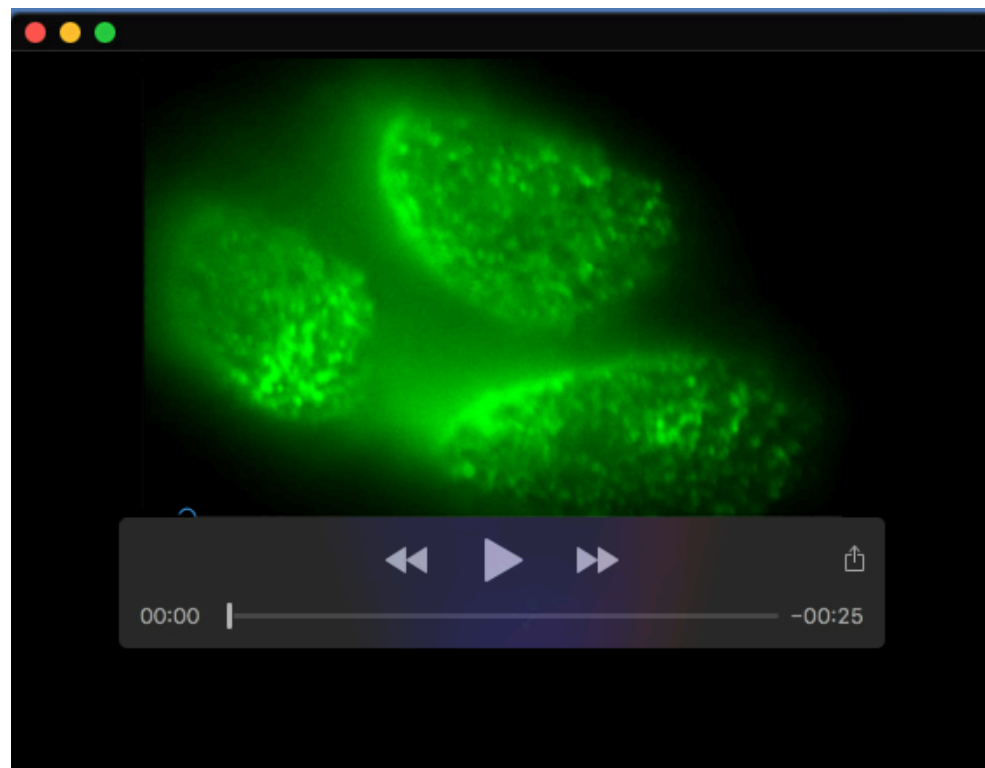
A) A plot shows the duration of ring assembly, furrow initiation and ring closure phases for individual control and *ran-3(RNAi)* AB and P₁ cells (average, red lines). B) Images show embryos co-expressing PGL-1::RFP and GFP::PH in 2-cell and 4-cell control (top) and *ran-3(RNAi)* (bottom) embryos. C) Images show divisions of AB and P₁ cells in control (top) and *ran-3(RNAi)* (bottom) embryos co-expressing mCherry-HIS::58, GFP::PH and GFP::TBB-2. D) Graphs show ring closure in AB (top) and P₁ (bottom) cells in control embryos or after *ima-3(RNAi)*, *imb-1(RNAi)* and *imb-1(RNAi); ima-3(RNAi)*. E) A western blot shows Myc-tagged importin- β from HeLa cell lysates (input) and after pull-down with recombinant, purified MBP or MBP-tagged ANI-1 (RBD + C2) containing mutations K938E; K940E or K947A; K949A. F) Inverted images show dividing AB (top) or P₁ (bottom) cells in embryos where endogenous ANI-1 is tagged with mNeonGreen (mNeonGreen::ANI-1), and after *ani-1(RNAi)* or *ran-3; ani-1(RNAi)*. The graphs show mNeonGreen::ANI-1 levels at the midplane cortex in control compared to RNAi-treated cells. All error bars show s.e.m. All scale bars are 10 μ m.

Table S1. *C. elegans* strains used in this study.

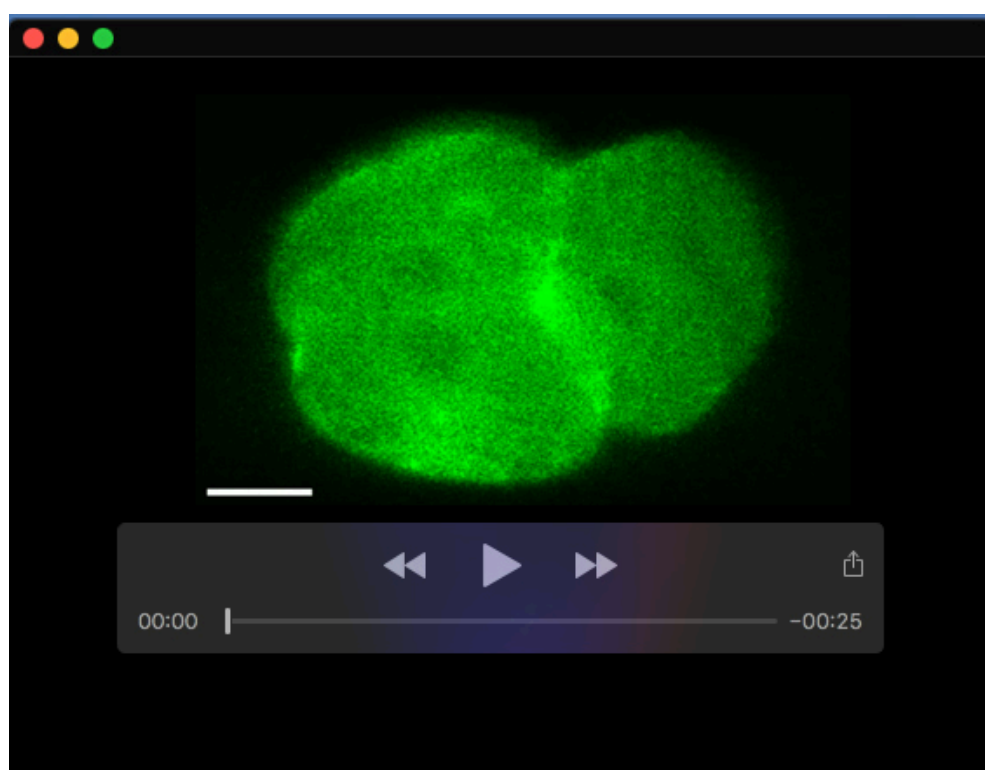
Strain	Genotype	Notes
UM463	<i>cpIs42[Pmex-5::mNeonGreen::PLCδ-PH::tbb-2 3'UTR; unc-119(+)] II;</i> <i>ltIs37[pAA64; Ppie-1::mCherry::HIS-58; unc-119(+)] IV</i>	Also used to generate a tetraploid strain.
OD95	<i>ItIs37 [(pAA64 Ppie-1::mCherry::HIS-58 + unc-119(+)]; ItIs38 [pie-1p::GFP::PH(PLC1delta1) + unc-119(+)] III</i>	
SWG001	<i>mex-5p::Lifeact::mKate2</i>	
LP162	<i>cp13[nmy-2::gfp + LoxP] I.</i>	Also used to generate a tetraploid strain.
MDX29	<i>ani-1(mon7[mNeonGreen^3xFlag::ani-1]) III</i>	



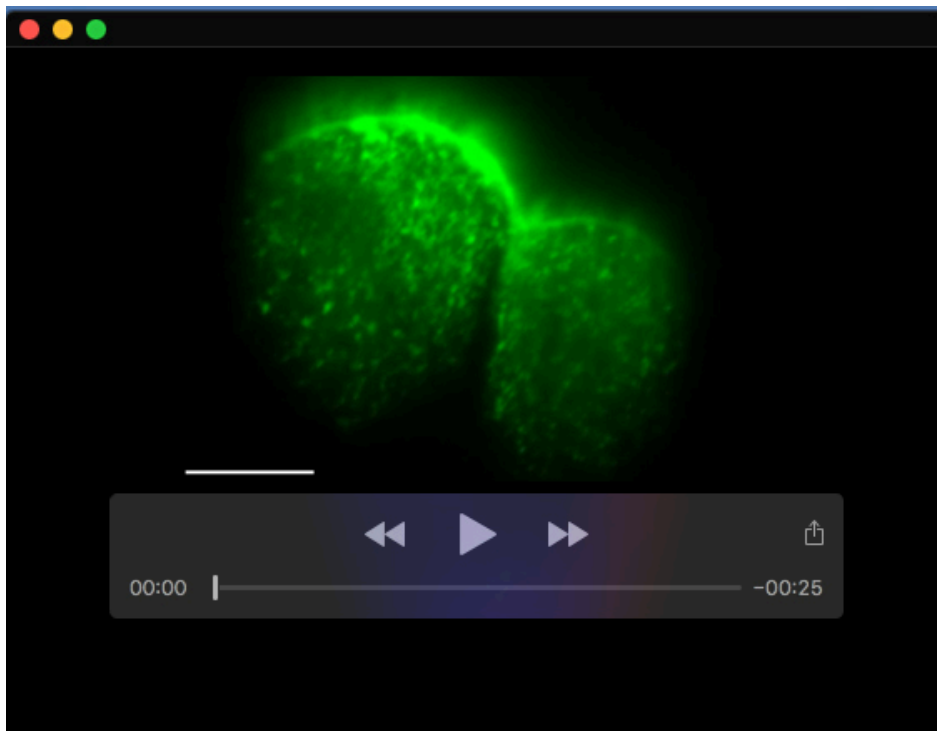
Movie 1. Timelapse images show HILO imaging of GFP::NMY-2 at the cortical surface of an AB cell during cytokinesis. Images were recorded at 2 second-intervals, with a playback rate of 7 frames per second, and the scale bar is 10 μm.



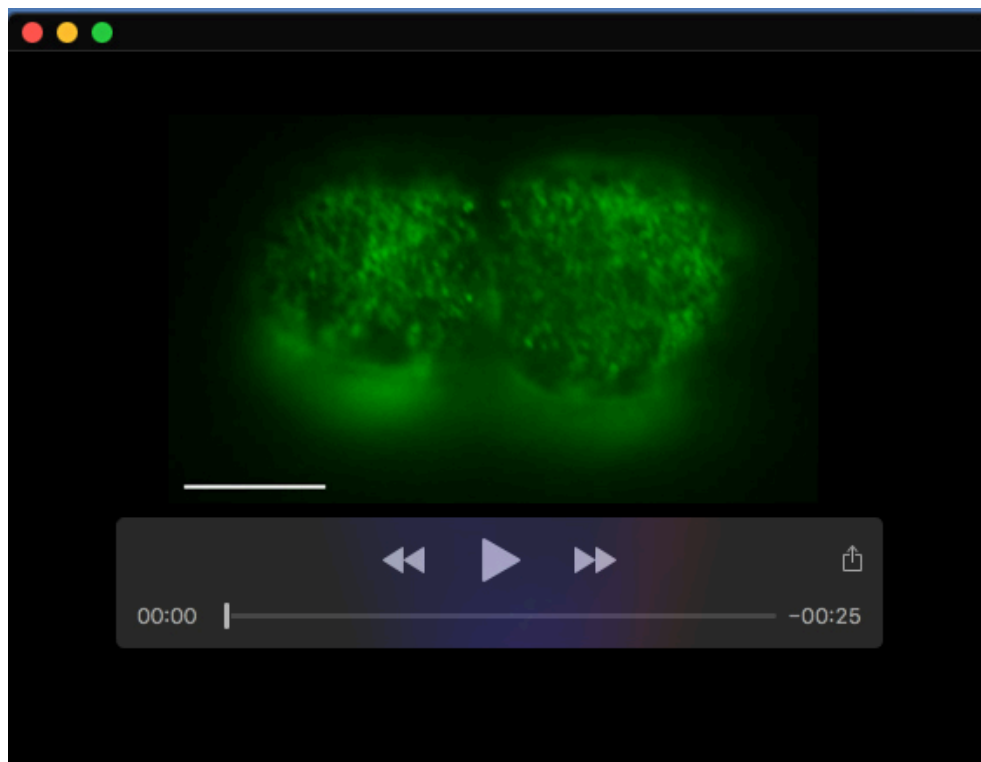
Movie 2. Timelapse images show HILO imaging of GFP::NMY-2 at the cortical surface of a P₁ cell during cytokinesis. Images were recorded at 2 second-intervals, with a playback rate of 7 frames per second, and the scale bar is 10 μm.



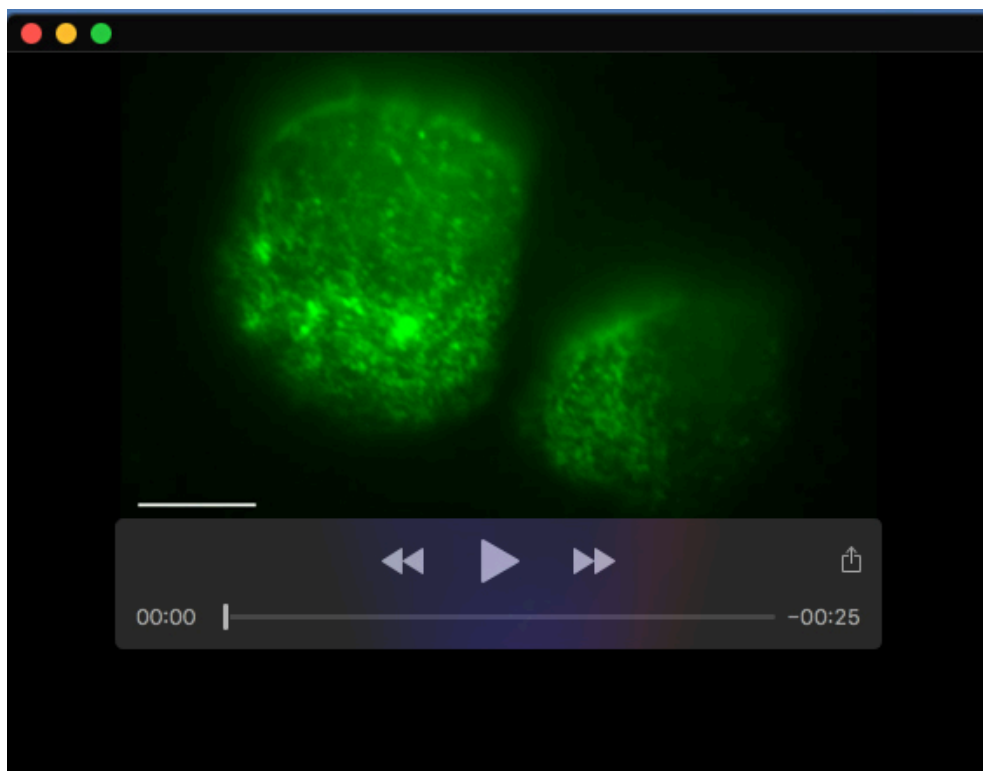
Movie 3. Timelapse images show confocal imaging of GFP::NMY-2 in *ect-2(RNAi)* AB (left) and P₁ (right) cells that fail cytokinesis. Images were recorded every 20 seconds, with a playback rate at 7 frames per second, and the scale bar is 10 μm.



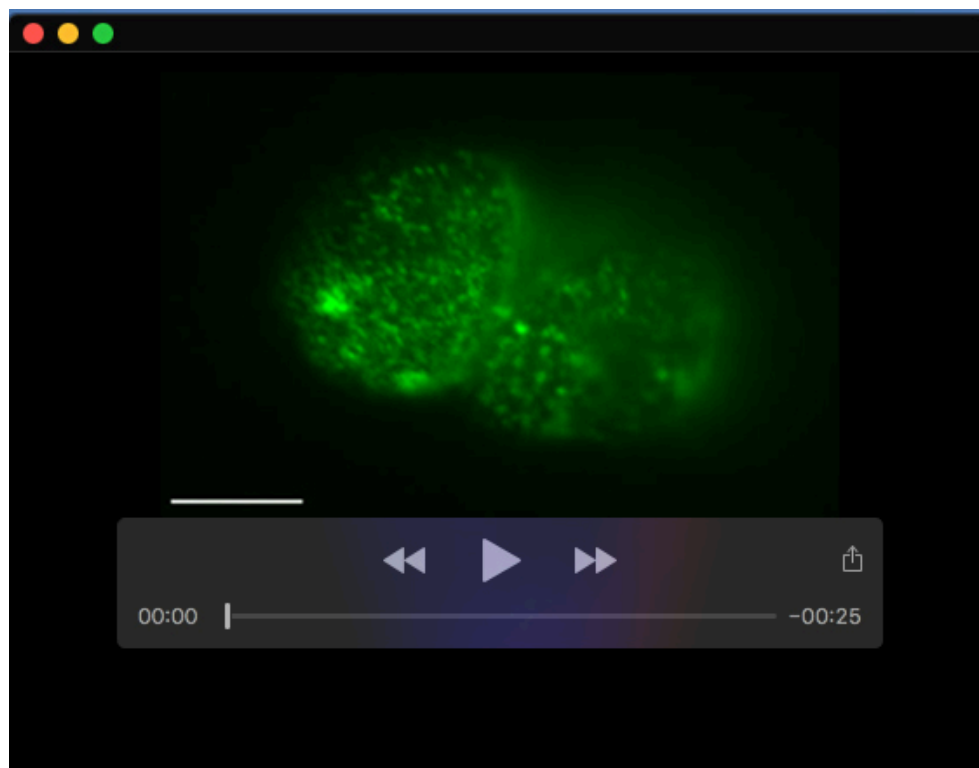
Movie 4. Timelapse images show HILO imaging of GFP::NMY-2 at the cortical surface of *ect-2(RNAi)* AB (top) and P₁ (bottom) cells during cytokinesis. Images were recorded at 2 second-intervals, with a playback rate of 7 frames per second, and the scale bar is 10 μm.



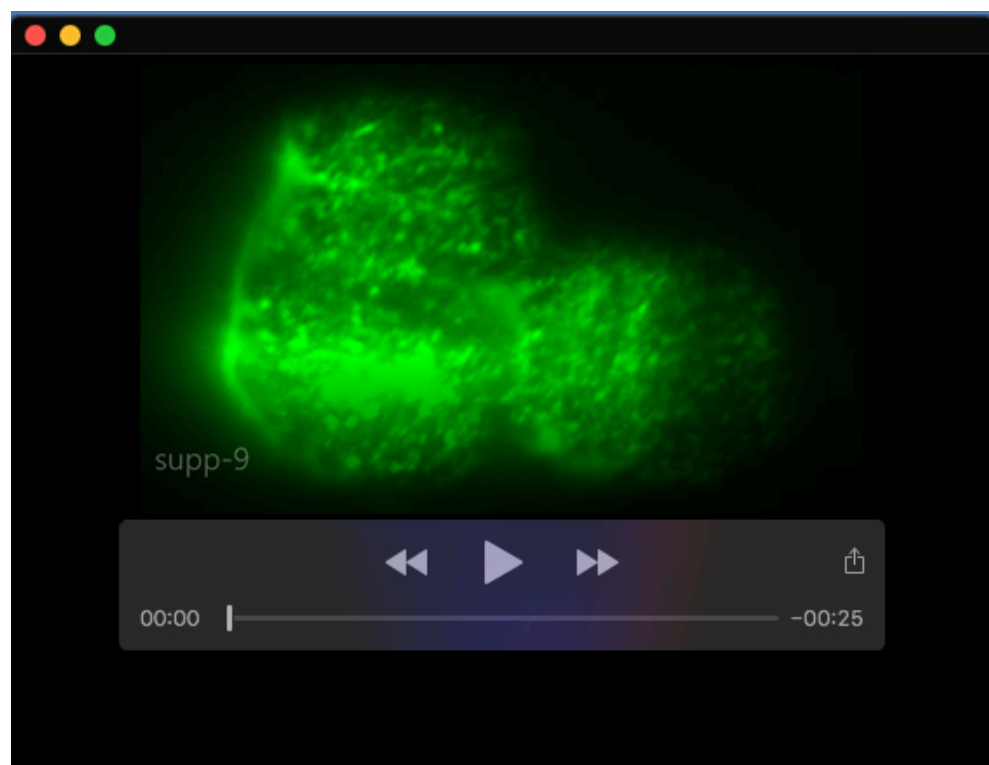
Movie 5. Timelapse images show HILO imaging of GFP::NMY-2 at the cortical surface of *par-1(RNAi)* P₀ daughter cells during cytokinesis. Images were recorded at 2 second-intervals, with a playback rate of 7 frames per second, and the scale bar is 10 μm.



Movie 6. Timelapse images show HILO imaging of GFP::NMY-2 at the cortical surface of tetraploid AB (top) and P₁ (bottom) cells during cytokinesis. Images were recorded at 2 second-intervals, with a playback rate of 7 frames per second, and the scale bar is 10 μm.



Movie 7. Timelapse images show HILO imaging of GFP::NMY-2 at the cortical surface of a *ran-3(RNAi)* AB cell during cytokinesis. Images were recorded at 2 second-intervals, with a playback rate of 7 frames per second, and the scale bar is 10 μm.



Movie 8. Timelapse images show HILO imaging of GFP::NMY-2 at the cortical surface of a *ran-3(RNAi)* P₁ cell during cytokinesis. Images were recorded at 2 second-intervals, with a playback rate of 7 frames per second, and the scale bar is 10 μm.